Antibacterial nanostructured composite coating on high performance Vectran™ fabric for aerospace structures

Antibacterial nanostructured composite coating on high performance Vectran™ fabric for aerospace structures

Cristina Balagna[a], Muhammad Irfan[a,b,*], Sergio Perero[a], Marta Miola[a], Giovanni Maina[c], Matteo Crosera[d], Daniela Santella[e], Antonia Simone[e], Monica Ferraris[a]

[a]*Department of Applied Science and Technology, Politecnico di Torino, Corso Duca degli Abruzzi 24,10129 Torino, Italy*

[b]*Department of Materials and Testing, National Textile University, Faisalabad, Pakistan*

[c]*Department of Clinical and Biological Sciences, Università di Torino, Via Zuretti 29, 10023 Torino, Italy*

[d]*Department of Chemical and Pharmaceutical Sciences, Università di Trieste, Via L. Giorgieri 1, 34127, Trieste, Italy*

[e] *Thales Alenia Space – Italy S.p.A., Strada Antica di Collegno 253, 10146 Torino, Italy*

[*]*Corresponding author:*

Tel: +92-41-9230081

Fax: +92-41-9230098

E-mail address: irfan@ntu.edu.pk

Abstract

Excellent mechanical, thermal and chemical properties make Vectran™ fibres an attractive material to be used in high end applications. Its aerospace applications, as in inflatable light weight habitat module, require functional coating to provide antibacterial protection to ensure safe environment for the astronauts. In this study, woven Vectran™ fabric was coated with an antibacterial silver nanoclusters/silica composite coating by means of radio frequency co-sputtering technique. The successful deposition of the silver nanoclusters embedded in the silica matrix of the composite coating was confirmed by morphological, compositional and structural analysis. The coating sustained 10 washing cycles with partial dissolution of the coating during washing. Silver leaching test verified the gradual and progressive release of ionic silver in aqueous media in the range 0.03 ppm - 0.43 ppm within 72 hours of immersion in water. Antibacterial properties of the coated Vectran™ fabric were confirmed in inhibition halo test against *Staphylococcus aureus* and *Escherichia coli* on as deposited as well as aged samples. An inhibition halo of up to 2 mm was observed for as deposited samples while after UV exposure, the samples formed inhibition halo of 4 mm. The percutaneous absorption test demonstrated a very low release of silver into epidermis and dermis. The effect of the coating on mechanical properties of the as deposited Vectran fabric was assessed through mechanical characterizations including tensile, tear and abrasion test.

Key words: co-sputtering, silver nano clusters, silica, antibacterial, coating, Vectran

1. Introduction

Vectran™ is a high performance thermotropic liquid crystal polymer fibre. It is an aromatic co-polyester of p-hydroxy benzoate (HBA) and 2-hydroxy-6-naphthoic acid (HNA) [1] and is melt spun into fibres at high temperatures. Highly oriented liquid crystal polymer domains along the fibre axis during extrusion results in a fibre with high tensile properties combined with lightness and flexibility [2]. Along with excellent mechanical properties including high strength-to-weight ratio and high abrasion resistance, Vectran™ also possesses thermal stability over wide temperature range, excellent chemical resistance, low moisture take up and no creep when loaded up to 50 % of its breaking strength [3]. Vectran™ exhibits much higher specific strength compared to titanium, stainless steel and aluminium. Because of these excellent properties, it finds its applications in numerous areas like ropes and cables, protective clothing, aerospace and medical devices [4]. In aerospace applications, it is used in astronauts' gloves as part of the outer thermal micrometeoroid garment (TMG) in the form of tricot knitted fabric [5] and in inflatable habitat systems. Vectran™ was used in air bags to help landing Mars Pathfinder on the surface of Mars in 1997 mission [4]. Vectran™ structural ribbons guarantee the specific mechanical behaviour during operation of space module recover after ditching. Bumper shields designed using Vectran™ fibres can provide lighter weight and thinner protection system having potential of being deployed to provide protection to the space infrastructure from the space debris [6].Medical applications include catheter reinforcement, actuation cables and device delivery systems [4]. Vectran™ fibres are very sensitive to UV radiation, which quickly deteriorate the mechanical properties of the material [7]. UV aging was found to cause 91 % decrease in the tensile strength of the fibres after 336 hours exposure to the UV lamp [1]. Several treatments as deposition of TiO_2 nanoparticle loaded coatings [8-10], have been reported in literature to improve the UV resistance of the Vectran™ fibres. Silver coating on Vectran™ fibres has been reported to decrease its electrical resistivity for potential application in the field of sensitive

electronic packaging [11]. Apart from these treatments, antibacterial coating for Vectran™ fibers becomes essential especially for medical and space applications.

The importance of antibacterial protection in space is eminent from the fact that several studies have confirmed the presence of different types of bacteria in space and reported their growth aboard [12-14], during space flights [15-17] and in the outer space environment [18]. A six-year study conducted on 554 samples collected from air and surfaces of International Space Station (ISS) reported a total of 36 bacterial and 32 fungal species recovered from surface samples whereas 15 bacterial and 5 fungal species recovered from air samples [12]. It was also reported recently that most of the built environment associated bacteria have similar growth behaviour and kinetics on ground as well as on board ISS. Since environmental conditions in ISS are maintained close to that of on earth, vast majority of bacteria behave similarly in space and on earth [19].

The presence of bacteria does not only pose health threats to the crewmembers but can also trigger degradation of engineering materials of the space station especially polymers. Some microbial species, that could potentially bio-deteriorate polymers and be potentially corrosive for metals, were also detected in space environment [12]. Although biodegradation rates are reported to be too slow to assess deterioration of structural integrity through available methods of mechanical characterization, polymeric materials used in electronics circuits and fibre reinforced composites are susceptible to bio-deterioration as they can support biofilm formation by providing organic carbon as a nutrition source [20].

During space missions, changes in immune system of the astronauts and the enhanced growth of bacteria both in liquid media in microgravity and in the internal environment of the space station can increase antibacterial threat [21]. Even if typical bacterial and fungal concentrations were found to be less than the acceptable threshold [12], the risk increases in long duration space missions due to crowded conditions and reclaimed water and air in the environment. However, effective prevention measures can lead to microbiologically safe environment in space [22]. The functionalization of surfaces with specific coatings for biodegradation reduction in internal space structures is of great interest to realize light space structure microbiologically safe for the crew and for every electrical system and cables that can be damaged by bacterial growth. However, coating of high performance fibres having chemically inert surfaces and higher crystalinity may be difficult via liquid based chemical processes involving organic reactions. Moreover, these processes may not be simple, involve multistep reactions along with use and release of environmentally hazardous chemicals [23]. On the other hand, plasma based processes (plasma sputtering, plasma polymerization) can effectively functionalize inert surfaces without influencing bulk properties of the materials [24]. In this study, woven Vectran™ fabric was coated with silver nanoclusters/silica composite coating through radio frequency (RF) assisted co-sputtering of silver and silica to impart antibacterial functionality. The antimicrobial performance of the composite coating has been verified and reported previously on various substrates including silica [25, 26], soda lime [27, 28], a multi-layered polymeric substrate [29], polypropylene prostheses [30], and ocular prostheses [31]. The coating has also demonstrated good thermal [26] and mechanical stability [29] as well as biocompatibility [30, 31].

2. Materials and Methods

2.1 Materials

Woven vectran™ fabric (textile weight of 240 ± 5% g/m^2, yarn count 2/26Nm and warp and weft density of 16 warps/wefts per inch, Iniziative Industriali Sas, Italy) was used as substrate. The composite coating comprising silver nanoclusters hosted in the silica matrix was deposited by means of radio frequency assisted co-sputtering technique. The sputtering equipment (Microcoat™ MS450) was equipped with two cathodes. For the co-sputtering process, one cathode was installed with silver target of 1 inch diameter and supplied by Sigma-Aldrich™ 99.99% purity and the other one with silica target of 6 inch diameter supplied by Franco Corradi S.r.l.™ 99.9% purity. Sputtering worked in pure argon atmosphere for 15, 40 and 80 minutes resulting in approximately 60, 150 and 300 nm thick coatings on the fabric surface as previously described in detail [27] [28]. For identification of the samples with different coating thickness, sputtering time has been added to the word "Vec" as suffix throughout in the article: Vec (control and uncoated sample), Vec_15 (15 minutes deposition), Vec_40 (40 minutes deposition) and Vec_80 (80 minutes deposition).

2.2 Coating morphology and composition

The coating morphology was investigated through Field Emission Scanning Electron Microscope (FESEM, QUANTA INSPECT 200, Zeiss SUPRATM 40™) which was equipped with Energy Dispersive Spectroscopy, (EDS, EDAX PV 9900™). For semi quantitative detection of elements, EDS scans were carried on three different sites of the samples at low magnification (250X). X-ray Photoelectron Spectroscopy (XPS, Phi 5000 Versa Probe™) was used to determine chemical states of the elements for coating composition analysis. For XPS, monochromatic Al Kα x-ray source with photon energy of 1486.6 eV at 15 kV and 1 mA was used. The binding energy scale was calibrated by setting the carbon C1s (C-C) binding energy at 284.5 eV. The operating condition was 21.7 W for the x-ray source and tilt angle for analyser was 45°. The survey scans were taken at pass energy of 187.85 eV with a step size of 1 eV whereas high resolution scans at pass energy of 23.50 eV with a step size of 0.1 eV.

2.3 Washing fastness

Coated Vectran™ samples of size 2.5 cm x 2 cm were washed in a detergent solution containing 100 ml of MilliQ water and 2 g/l of a commercial detergent (castile soap with sodium bicarbonate). Washing was carried in thermostatic bath at 60 ˚C for 30 minutes with an oscillation of 150 rpm. The samples were rinsed with distilled water after washing and dried at room temperature. Washed samples were analysed through FESEM and EDS

2.4 Silver leaching test

Silver leaching test in water was performed to assess the ionic silver release from the coated Vectran™ samples. The coated samples of 1cm^2 were submerged in a container filled with 25 ml of water (MilliQ) with coated side faced up. Ionic silver content was measured after 3, 24 and 72 hours of sample immersion using silver photometer (Hanna Instruments™). The test was carried in triplicate for each coating thickness.

2.5 Antibacterial test

Antibacterial properties of the coated samples were verified through inhibition halo test according to the National Committee for Clinical Laboratory (NCCLS) standard [32]. The test was done against *Staphylococcus* aureus, a Gram positive bacterium and *Escherichia coli* a Gram negative bacterium. A

standard inoculum of bacteria was prepared by dissolving the bacterial colonies, picked from a pre cultured blood agar plate, in the physiological solution and adjusting its turbidity index (McFarland Index) to 0.5. The bacterial inoculum was then uniformly swabbed on the surface of Muller Hinton agar and coated Vectran^{TM} samples (of size 1 cm^2) were placed on the surface of the agar such that the coated side of the fabric was in contact with the bacterial suspension. The agar plates were incubated at 35 °C for 24 hours to allow bacterial growth. The antibacterial effect was assessed by evaluating the agar plates after incubation for the formation of the inhibition halo which is an area around the samples where bacteria did not grow.

2.6 Percutaneous test

Percutaneous test, using Franz static diffusion cell method, evaluates the permeation of silver into the skin [33]. Vec _40 were selected for this test and a comparison with the UV aged samples was performed. The cryopreserved skin was previously obtained from the back and arms of two donors [34]. In the static diffusion cell, the skin, with an exposed area of approximately 3.3 cm^2 and a thickness of about 0.5 mm, was clamped between the donor and the receptor compartment. The measurement of electrical conductibility monitored skin integrity before and after the experiment. Values of resistance less than 3.95 ± 0.27 kΩ cm^{-2} indicate the damage of the skin with consequent preclusion to use it [35]. Two coated Vectran samples (area of 4 cm^2) were soaked into 4 mL of synthetic sweat (composition: 0.5 % sodium chloride, 0.1 % urea, and 0.1 % lactic acid, in Milli-Q water, with ammonium hydroxide to reach a pH of 4.5) in the donor chamber. Only synthetic sweat was added into other cell as control.
The physiological solution (2.38 g of Na_2HPO_4, 0.19 g of KH_2PO_4, and 9 g of NaCl dissolved in 1 L of Milli-Q water, with a final pH of 7.35) was used as receiving phase fluid in the receptor compartment and continuously mixed using a Teflon-coated magnetic stirrer at a temperature of +32 °C. The salt concentration of the receptor fluid simulates the salt concentration of human blood. Silver concentration permeated in the receptor compartment was evaluated during 24 hours of immersion, sampling and analysing 1.5 mL of receiving phase at selected intervals (8, 16, 20, 24 hours). At any time, an equal amount of fresh physiological solution was added to the initial solution. The experiment was repeated twice. After 24 hours, Vectran ^{TM} samples were removed from the synthetic sweat and skin samples were washed with Milli-Q water to remove any excess of silver from the surface. For the skin mineralization, dermis and epidermis were separated by immersion in hot water (+60 °C) for 1 minute, dried in oven for 24 hours and immersed into1 mL of HNO_3 69% v/v for mineralization. The permeation test has been repeated using aged Vec_40 in the donor chamber.
Inductively Coupled Plasma Mass Spectrometry (ICP-MS, NEXION 350D, Perkin Elmer) with an integrated auto sampler was used to determine the concentration of the silver in the receptor and donor fluids as well as in the skin after mineralization.

2.7 Mechanical test

The mechanical characterization of the Vectran fabric (both coated and uncoated), were evaluated by means of tensile [36], tear [37], and abrasion [38] tests according the respective standards. These tests were performed to assess whether the mechanical properties of the Vectran fabric were intact or influenced by the deposition process. Tensile and tear resistance were assessed both along the warp and weft directions of the fabric. Samples for tensile test were smaller than that mentioned in the standard (100x80 mm instead of 100x150mm) because of limited dimensions of sputtering chamber.

2.8 UV-Ageing treatment

Uncoated and coated Vectran^{TM} (only Vec_40) was exposed to UV radiation at 50 W/m^2 for 5 h within a wavelength range of 185-254 nm (Elios Ital Quartz with UV lamp Hg typed P) (*in the text UV*). The aged samples were analysed in terms of antibacterial performance, percutaneous absorption and mechanical properties.

3. Results and discussion

3.1 Morphological and compositional analysis

The morphology of uncoated and coated Vectran^{TM} fibres is shown in FESEM images in Figure 1. FESEM images at high magnification show that uncoated Vectran^{TM} fibres have relatively smooth surface whereas coated fibres surface is rougher. The sputtering parameters of both silica and silver are optimized in such a way that result in uniform and homogeneous distribution of silver in the form of nanoclusters that are hosted in the silica matrix. A glimpse of such distribution is depicted in Figure 2 which FESEM image taken in back scattered mode. The silica matrix of the coating firmly embeds silver nanoclusters and grows in a globular form with increased deposition time (Vec_40). This structure seams to coalesce with further increase in deposition time (Vec_80) thus relatively smoothening the granular surface appearance. The golden colour of the uncoated Vectran^{TM} fabric changed after the deposition. At lower coating thickness, the fabric assumed light brown color that turned into dark brown with increased coating thickness. The change in color occurred due to the Localized Surface Plasmon Resonance (L–SPR) related to the silver nanoclusters [29, 39]. The XRD of the composite coating deposited on the silica substrate, reported and discussed previously [26], also confirmed that coating was composed of metallic silver and amorphous silica matrix.

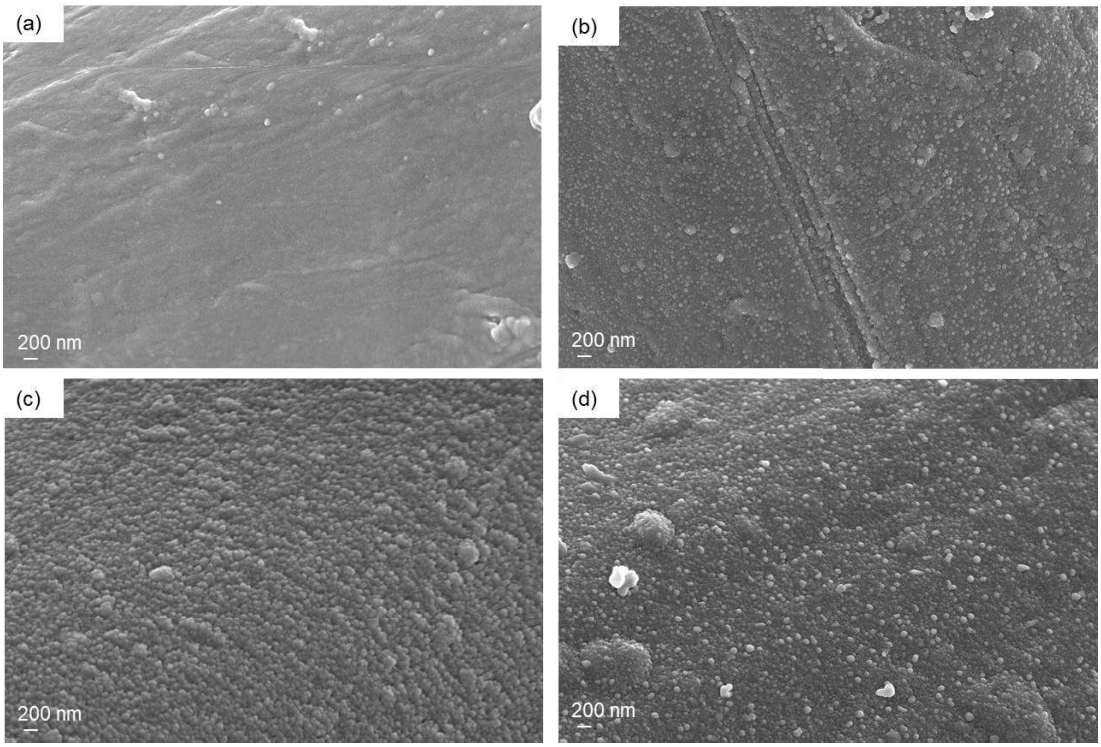

Figure 1. FESEM images of Vectran^{TM} fibres: (a) uncoated and after (b) 15, (c) 40 and (d) 80 min deposition of showing morphology of the composite coating.

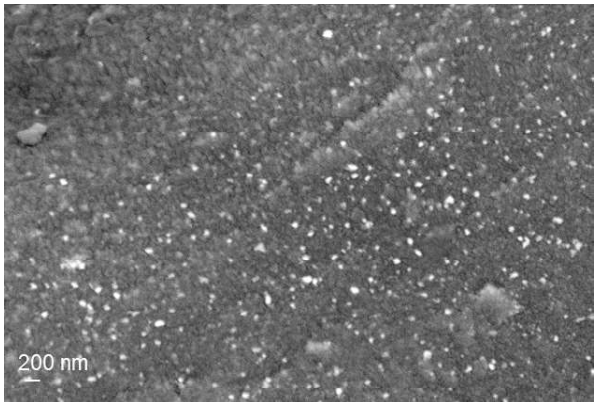

Figure 2. FESEM images of Vec_80 in BSE mode: some silver nanoclusters as bright dots can be seen on the coated fibre surface

Figure 3 reports EDS spectra of the uncoated and coated samples. The spectrum of uncoated fibres consists of C and O peaks whereas Ag and Si peaks appear after deposition of silver nanoclusters/silica composite coating. Cr peaks are present due to Cr coating needed for the FESEM analysis. The atomic percentage ratio Ag/(Ag+Si) was calculated and reported on the respective EDS spectrum. The ratio is fairly constant and remains within values 0.36 – 0.39 for the three depositions. The ratio represents average values obtained from three different EDS scans on the sample surface at low magnification (at 250X) to collect information from wider surface area. This implies that the co-deposition technique was

reproducible and the contents of Ag and SiO_2 of the composite coating can be controlled individually to achieve a desired ratio between them.

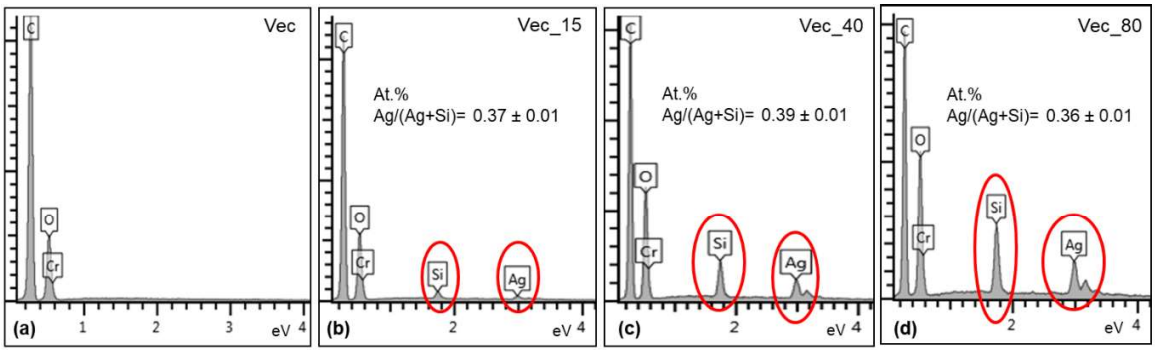

Figure 3. EDS spectra and relative atomic% ratio between Si and Ag of (a) Vec, (b) Vec_15, (c) Vec_40, (d) Vec_80

XPS investigations were carried on Vectran fabric before and after coating deposition (only Vec_40 and Vec_80) and results are shown in Figure 4. The survey spectrum of uncoated fibres consists of C-1s and O-1s peaks. Ag-3d, Si-2s and Si-2p peaks emerge after the deposition of the composite coating. The high resolution spectra of the four individual chemical elements C, O, Ag and Si are given in Figure 5. The C-1s peak of the uncoated Vectran^{TM} fibre is a convolution of the three sub peaks. The sub peak at binding energy 284.8 eV is representative of C-C bonds. The sub peaks at 286.3 eV and 288.9 eV can be attributed to C-O and –COO- groups respectively present in the molecular structure of the Vectran^{TM} fibres [1]. The Ag-3d doublet, with two states at binding energies of 374.2 eV and 368.2 eV, is referred to Ag-$3d_{3/2}$ and Ag-$3d_{5/2}$, respectively representing silver in the metallic state [28]. The silver 3d peaks for Vec_80 are at slightly higher binding energy (0.2 eV) as compared to those of Vec_40, this is probably due to the difference in the thickness of the silica matrix. However, the splitting between Ag-3d doublet in both the cases is 6 eV which shows silver is in Ag^0 state. The same has been observed and reported in literature when silver particles were embedded in TiO_2 matrix [40]. The O-1s peak appears at 532.7 eV and is indicative of oxygen bonded to silicon with Si-2p peak at 103.3 eV representing silica [41].

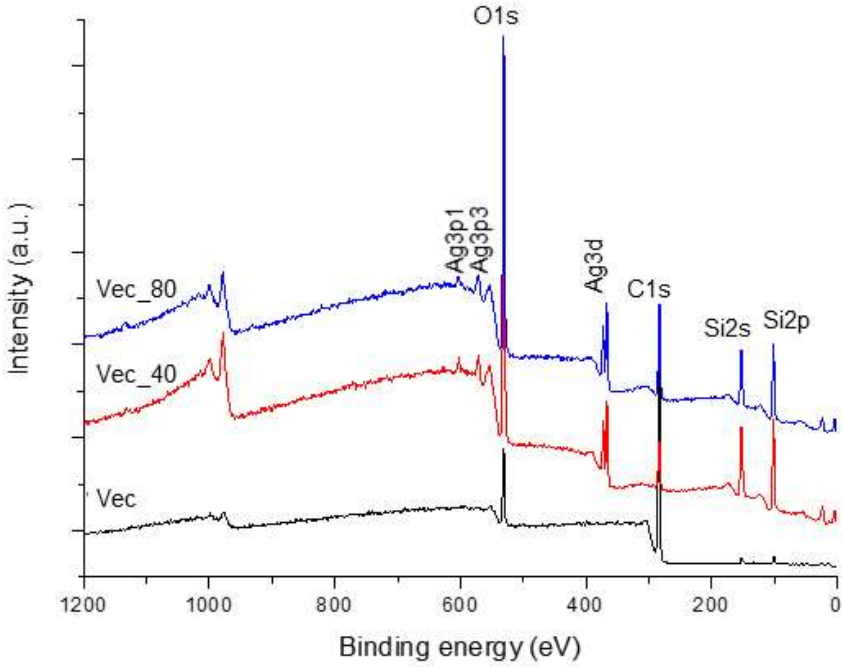

Figure 4. XPS survey spectra of uncoated (Vec) and coated (Vec_40 and Vec_80) Vectran™ fibres.

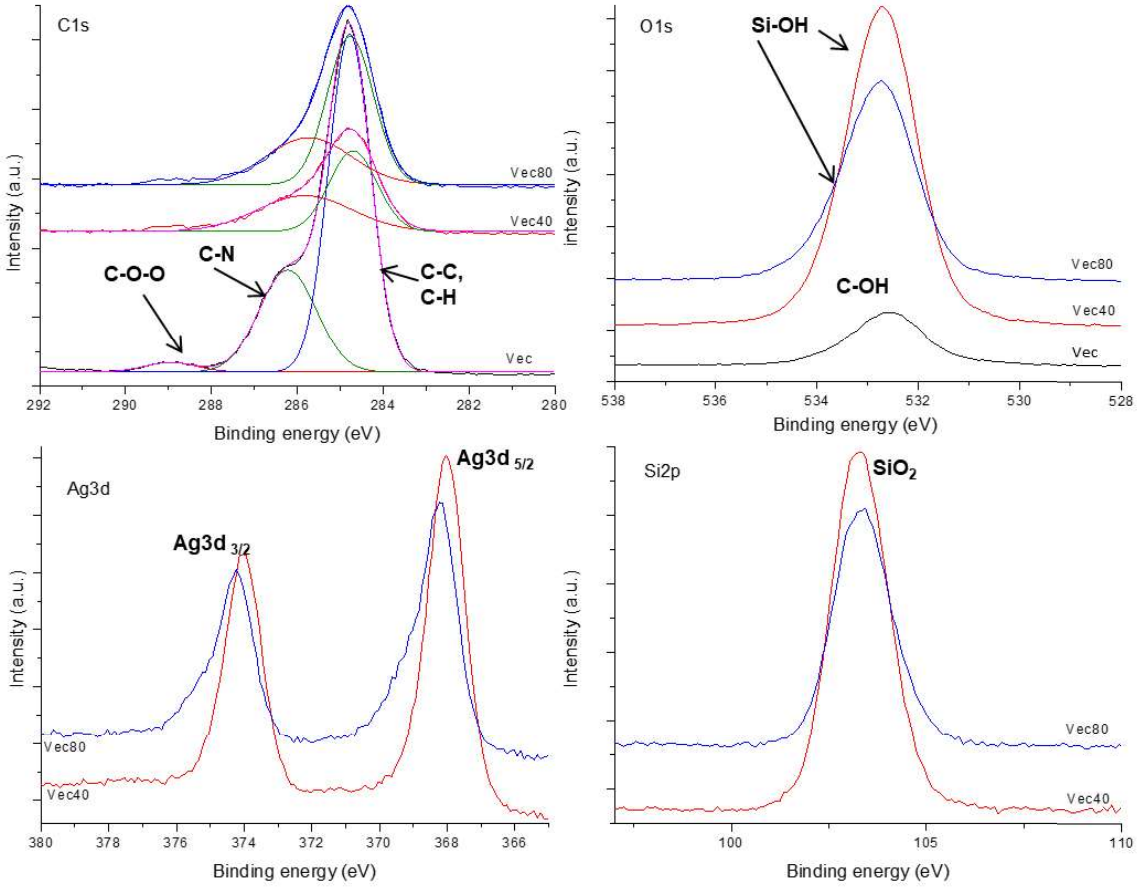

Figure 5. High resolution XPS spectra of C-1s, O-2s, Ag-3d and Si-2p peaks of uncoated (Vec) and coated (Vec_40 and Vec_80) Vectran™ fibres.

3.2 Washing Fastness

Washing stability of the coating on Vec_40 samples was assessed in multiple washing cycles and samples were analysed through FESEM and EDS after 1, 5 and 10 washing cycles. Figure 6 shows the FESEM image along with EDS spectrum of a 10 times washed sample. It can be seen that silver nanoclusters, visible as bright particles on the surface of the fibres, were still present after 10 washes. EDS spectrum also confirms the presence of Si and Ag on washed samples. The washing resistance of the coating is important for prolonged antibacterial functionality. Partial dissolution of the coating is also evident from the comparison of the FESEM images and EDS spectrum of as deposited samples in Figures 1 and 3 (Vec_40) with that of washed sample. It is worth noting that in aerospace applications (intended application for this study) washing of the structural parts and surfaces made of high performance fibres is not required or is less frequent.

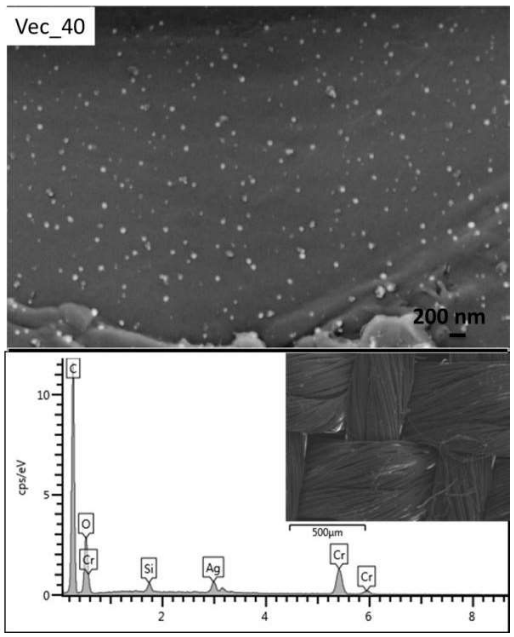

Figure 6. FESEM image (in back scattered mode) and EDS spectrum of Vec_40 after 10 washing cycles.

3.3 Silver leaching test

Silver nanoclusters get oxidized when in contact with aqueous media and release silver ions in the surrounding environment. Silver ions can react with phosphorus moieties in DNA and sulphur containing proteins in bacterial cell membrane and thus cause antimicrobial action [42]. Therefore, silver leaching test was performed to study the ionic silver release behaviour of the composite coating in water. The release kinetics of cumulative silver ions after being immersed in water for 3, 24 and 72 hours are shown in graph in Figure 7. Higher the coating thickness, higher was the concentration of the ionic silver released in the water. However, the comparison of the curves shows that silver ions did not release abruptly, rather they released progressively over the period of sample immersion which is a good aspect for sustained antimicrobial activity. The amount of ionic silver released within 72 hours was in the range between 0.03 mg/l/cm^2 (0.03 ppm) and 0.43 mg/l/cm^2 (0.43 ppm) which is higher than the minimum concentration considered necessary to cause antibacterial action [43]. The chemistry of the underlying fibres may influence the amount of silver ions released from the composite coating. Silver ion release profiles of the present study are similar to what has been reported previously for cotton fabric [44] but different from that of Kevlar fabric [45]. The graph shows a gradual and time dependent release of silver ions which is good aspect for sustained antibacterial effect. An abrupt release of silver from the coating will deprive the fabric of the antibacterial effect of the composite coating.

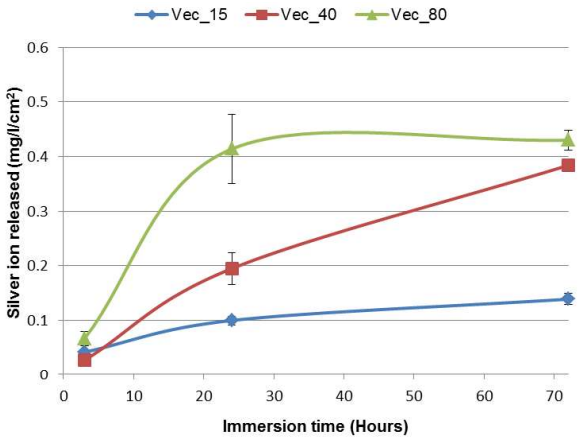

Figure 7. Silver leaching test showing cumulative ionic silver released in water over time from the coated samples (Vec_15, Vec_40 and Vec_80)

3.4 Antibacterial test

The antibacterial performance of the composite coatings was assessed through inhibition halo test against *Staphylococcus aureus* (a Gram positive bacterium) the most commonly involved bacterial strain in infection development [46]. The photographs in Figure 8 show that the coated samples exhibit antibacterial activity against *S. aureus* by forming an inhibition halo around them with size depending on the coating thickness and hence on the silver content. Less than 1 mm non uniform inhibition halo is formed around the samples Vec_15 and Vec_40. The size of the inhibition halo increased up to 2 mm around Vec_80. The intensity of the antibacterial activity increased with increase in coating thickness. If the coating thickness increases, the amount of silver in the coating as well ionic silver released from the composite coating also increases. As a consequence, the inhibition halo is higher at higher coating thickness. As the silica forms a porous matrix, silver ions are released also from nanoclusters positioned in the innermost layers of the matrix. So thicker coating shows an improved antibacterial effect.

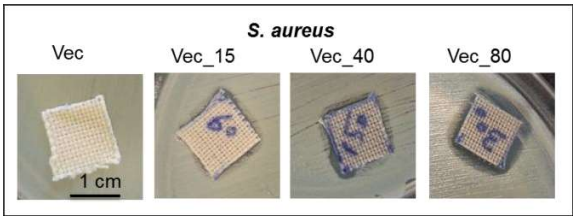

Figure 8. Antibacterial inhibition halo test against *S. aureus* on coated Vectran™ (Vec_15, Vec_40 and Vec_80), compared with the uncoated fabric (Vec)

Further investigations on Vec_40 sample were performed analysing the sample towards *Escherichia coli* (a Gram negative bacterium) and towards *Staphylococcus aureus* after UV ageing treatment (Figure 9). Against *E. coli*, Vec_40 exhibited antibacterial effect by forming an inhibition halo of 1 mm around Vec_40 as reported in Figure 9. The inhibition halo was less transparent in case of *E. coli* due to growth of some bacterial colonies within the inhibition zone. However, no *E. coli* colonies grew under the surface of the coated samples unlike control where growth of bacterial colonies is visible in the image showing back agar surface.

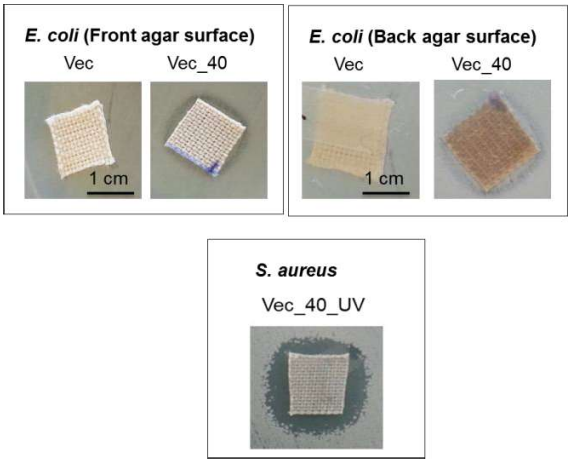

Figure 9. Antibacterial inhibition halo test of Vec_40: (a) against *E.coli* compared with the uncoated fabric (Vec), (b) against S. aureus after UV ageing

Finally, Vec_40 samples was subjected to UV ageing for 5 h and the antibacterial test is reported in Figure 9. The figure shows that the size of the inhibition halo formed around UV aged sample is maximum (4 mm) as compared to that of around other samples. This difference in the antibacterial activity could be due to different release of Ag^{+} from the composite coating. Since silver ions are considered to be responsible for the antibacterial activity of silver nano particles/clusters, any increase or decrease in the release of silver ions from the coating can increase or decrease the intensity of the antibacterial action. Studies in literature have reported an increase in the kinetics of silver ion release from silver nanoparticles under UV irradiation [47] [48] which could be the reason of enhanced antibacterial activity of Vec_40 samples after UV exposure.

3.5 Percutaneous test

The starting concentrations of silver were similar into the coatings on Vec_40 samples and they resulted: 59 ± 6 μg/g in Vec_40; 55 ± 26 μg/g in Vec_40_UV. The permeation profile of the silver released into synthetic sweat from the Vec_40 samples (both not aged and aged) is reported in Figure 9. At 24 hours, the total amount permeated in the acceptor compartment has a very low range, between 1-2.5 ng/cm^2, although cells exposed to aged Vec_40 reach a plateau after 8 hours, while in those exposed to not aged sample silver permeation starts later and it becomes comparable to the first only after 16 hours of exposure. This is probably due to a greater concentration of free Ag in the donor phase. Infact the analysis of the synthetic sweat, at the end of the 24 hours, showed a greater ionization for aged fabrics compared to the non-aged ones (13.1% vs 3.6%).

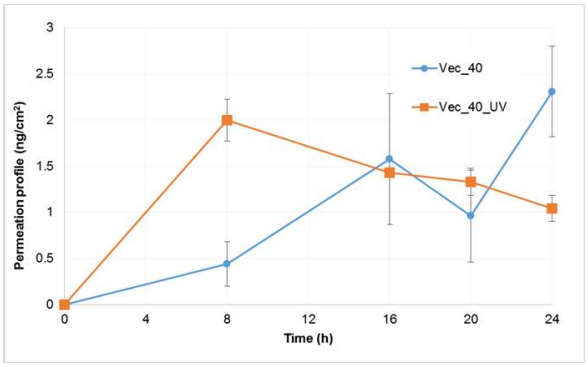

Figure 10. Permeation profile of silver release in synthetic sweat

Figure 11 provides the histogram relative to the silver penetration into epidermis and dermis. First of all, it is possible to notice two features: the higher amount of silver penetrated in the epidermis than the value in the dermis and the influence of ageing treatment which increase the amount of penetration with respect to the not aged sample. Dermal absorption data are in good agreement with those of other ex vivo experiments showing the same behaviour [49] a quite constant permeation in the ng/cm^2 range and a penetration into the skin layers depending on the Ag^+ release in the donor compartment. The epidermis, and in particular the stratum cornea, can reduce the amount of silver available for the penetration and systemic uptake through the reaction of silver ions with different functional groups of proteins and free amino acids, especially those containing sulphur [50]. So an increased silver dose could result in a higher concentration in the skin but not in the receiving phase.

All the data result negligible in terms of human safety. In fact, coated Vectran ^{TM} is not in close contact for a prolonged and continuous time (24h) with the crewmember's human skin.

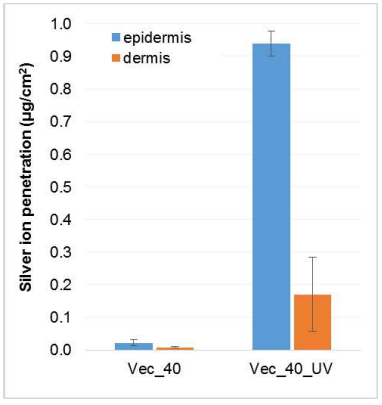

Figure 11. Histogram relative to the silver permeation into epidermis and dermis

3.6 Mechanical test

The mechanical properties of the substrate fabric may be deteriorated during coating deposition either due to the chemicals used or by the stresses the fabric has to go through during coating process. *Cheng et al.*

reported 45% reduction in the tensile strength of the cotton fabric after application of chitosan based antibacterial coating on the fabric [51]. Therefore, mechanical properties of the uncoated and coated Vectran^{TM} fabric were examined in terms of tensile and tear strength, both in warp and weft direction, and abrasion resistance for 50,000 abrasion cycles, before and after UV ageing treatment. The results of tensile and tear tests are shown in Figure 12. A comparison of the results of uncoated (Vec) and coated (Vec_40) fabric, without any ageing treatment ("*no ageing" in the graph*), shows that tensile and tear strength, both in warp and weft direction, was slightly improved after coating. This is probably due to the increased fibre to fibre friction after deposition of nanostructured coating. It should be noted that untreated Vectran^{TM} fibres have smoother surface, therefore, any roughness introduced on the fibre surface either by etching or coating can increase inter fibre or inter yarn friction which can potentially improve mechanical properties. It has been reported in literature that the tensile properties of fabric made of Kevlar fibres, another high performance fibre with smooth surface, were appreciably improved after simple plasma etching and were three folds increased after plasma deposited coating [24]. The Figure 12 shows that Vectran^{TM} demonstrated a significant decrease in the mechanical properties after UV aging and the presence of coating was not able to stop UV deterioration. It was demonstrated that the UV irradiation can induce Vectran^{TM} fibre bond chain scissions with more effect in air [1]. In this case, the coating is not sufficient to protect the fibres from the UV degradation in the wavelength range of 185-254 nm.

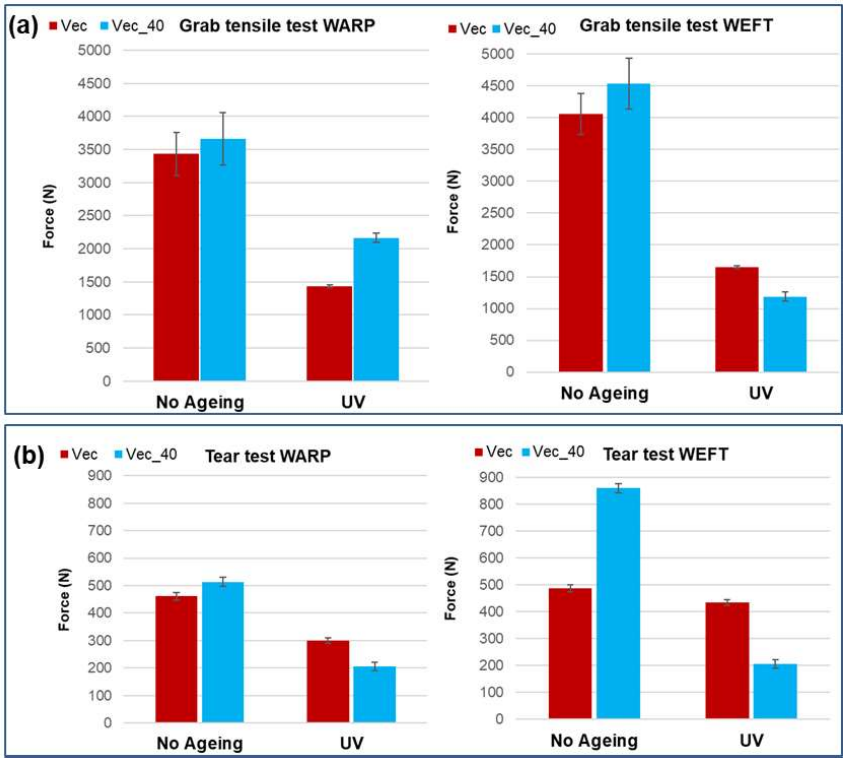

Figure 12. Histograms showing tensile and tear test results for uncoated and coated fabric both in warp and weft direction of the fabric, before and after UV ageing

In abrasion test (not reported here), both coated and uncoated fabric did not show any sign of failure when subjected to 50,000 abrasion cycles. It can be concluded from these results that the coating deposition process itself did not deteriorated any mechanical properties of the fabric as is reported for some other

finishing processes in literature [51]. Rather coated Vectran™ fabric demonstrated improved tensile and tear performance. However, Vectran ™ fibres normally suffer from UV radiation and the silver nanocluster/silica composite coating is not able to protect the fibres under UV radiation. Preserving (or enhancing) mechanical properties of high performance fibres during surface functionalization is of utmost importance for demanding applications, for example, in structural parts for space applications.

Conclusions

Antibacterial silver nanoclusters/silica composite coating was successfully deposited using RF co-sputtering on high performance woven Vectran™ fabric intended for aerospace applications. The deposition via RF co-sputtering resulted in reproducible composite coating composed of silver nanoclusters embedded in the silica matrix and distributed uniformly over the surface of the fibres as confirmed by FESEM, EDX and XPS. The coating showed good washing durability as it was still present after 10 washing cycles. Progressive release of silver ions (in the range 0.03 ppm - 0.43 ppm) from the composite coating was observed during leaching test within 72 hours of continuous immersion in water. The study suggests that sputtering can be used as an effective coating technique, alternative to the wet processes and treatments, to deposit functional coatings on technical and high performance textiles. The composite coating exhibited antibacterial properties by forming inhibition halo of up to 2 mm against *S. aureus* and *E. coli* in the inhibition halo test. The coated fabric was able to retain its antibacterial properties when subjected to UV aging. After UV exposure, the size of the inhibition halo was 4 mm. The skin permeation test showed that the amount of silver permeated into the skin can be considered negligible for the human safety even if it increased after the exposure to UV radiation. Coating deposition did not negatively influence the mechanical properties of the textile. An improvement in the tensile and tear strength of the fabric was observed after deposition of the coating due to surface roughening of coated fibres. However, it was demonstrated that the coating was not able to decrease mechanical deterioration after UV aging. Our findings demonstrate that an effective, homogeneous and conformal antibacterial coating can be deposited on high performance textiles via eco-friendly sputtering technique while preserving their mechanical properties.

Acknowledgments

This study was sponsored by Regione Piemonte and Polo Innovazione Tessile – Italy. The project title was "MARTe: Materiali Antibatterici per il Rivestimento di Tessuti" (Program: PAR-FSC 2007-2013 - Asse I – Innovazione e transizione produttiva, no GA number). The cooperation of Thales Alenia Space-IT and Iniziative Industriali sas, project partners, and Dr. Giacomo Fucale (Traumatology Orthopaedics and Occupational Medicine Department) is highly acknowledged.

References

[1] Y Liu, Y Liu, H Tan, C Wang, H Wei, Z Guo, Structural evolution and degradation mechanism of Vectran fibers upon exposure to UV-radiation, Polymer Degradation and Stability 98 (2013) 1744-1753.

[2] C.K Saw, G Collins, J Menczel, and M Jaffe, Thermally induced reorganization in LCP fibers - Molecular origin of mechanical strength, Journal of Thermal Analysis and Calorimetry 93 (2008) 175–182.

[3] D.E Beers and J.E Ramirez, Vectran high-performance fibre, The Journal of Textile Institute 81 (1990) 561-574.

[4] http://www.vectranfiber.com/

[5] D.A Shockey, R.S Piascik, B.J Jensen, and L.S, Sutter, J.K Hewes, Textile Damage in Astronaut Gloves, J Fail. Anal. and Preven. 13 (2013) 748–756.

[6] M Tanaka and Y Moritaka, Single bumper shields based on Vectran fibers, Advances in Space Research 34 (2004) 1076–1079.

[7] M.A Said, B Dingwall, A Gupta, A.M Seyam, G. Theyson, T Mock, Investigation of ultra violet (UV) resistance for high strength fibers, Advances in Space Research 37 (2006) 2052–2058.

[8] Y Liu, Y Liu, C Zhang, H Tan, X Yan, H Wei, Z Guo, Hyperbranched polyester-stabilized nanotitania-coated vectran fibers with improved uv-blocking performance, Macromolecular Materials and Engineering 300 (2015) 64–69.

[9] J Won, M.A Said, A.M Seyam, Development of UV protective sheath for high performance fibers for high altitude applications, Fibers and Polymers 14 (2013) 647-652.

[10] Y Liu, Y Liu, J Lin, H Tan, C Zhang, UV-protective treatment for Vectran® fibers with hybrid coatings of TiO2/organic UV absorbers, Journal of Adhesion Science and Technology 28 (2014) 1773-1782.

[11] X Xia, H Wang, F Huang, Y Cai, Q Wei, Surface characterization of aromatic thermotropic liquid crystalline fiber deposited by nanostructured silver, Fibers and Polymers 11 (2010) 813-818.

[12] N Novikova P De Boever, S Poddubko, E Deshevaya, N Polikarpov, N Rakova, I Coninx, M Mergeay, Survey of environmental biocontamination on board the International Space Station 157 (2006) 5-12.

[13] Y Kawamura, Y Li, H Liu, X Huang, Z Li, T Ezaki, Bacterial Population in Russian Space Station "Mir", Microbiology Immunology 45 (2001) 819-828.

[14] V.A Castro, A.N Thrasher, M Healy, C.M Ott, D.L Pierson, Microbial characterization during the early habitation of the international space station, Microbial Ecology 47 (2004) 119–126.

[15] A Crabbe′, M.J Schurr, P Monsieurs, L Morici et al., Transcriptional and proteomic responses of pseudomonas aeruginosa pao1 to spaceflight conditions involve hfq regulation and reveal a role for oxygen, Applied And Environmental Microbiology 77 (2011) 1221–1230.

[16] W Kim, F.K Tengra, J Shong, N Marchand et. al., Effect of spaceflight on Pseudomonas aeruginosa final cell density is modulated by nutrient and oxygen availability, BMC Microbiology 13 (2013) 1-10.

[17] D Klaus, S Simske, P Todd, L Stodieck, Investigation of space flight effects on Escherichia coli and a proposed model of underlying physical mechanisms, Microbiology 143 (1997) 449-455.

[18] N Novikova, E Deshevaya, M Levinskikh, N Polikarpov, S Poddubko, Study of the effects of the outer space environment on dormant forms of microorganisms, fungi and plants in the 'Expose-R' experiment, International Journal of Astrobiology 14 (2015) 137–142.

[19] D.A Coil, R.Y Neches, J.M Lang, W.E Brown et al., Growth of 48 built environment bacterial isolates on board the International Space Station (ISS), PeerJ (2016) 1-11.

[20] J-D Gu, Microbial colonization of polymeric materials for space applications and mechanisms of biodeterioration: A review, International Biodeterioration & Biodegradation 59 (2007)170–179.

[21] L.A Mermel, Infection prevention and control during prolonged human space travel, Healthcare Epidemiolgy 56 (2009) 123-130.

[22] D.L Pierson, Microbial contamination of spacecraft, Gravitational and Space Biology Bulletin 14 (2001) 1-6.

[23] M Widodo, A El-Shafei, P.J Hauser, Surface nanostructuring of Kevlar fibers by atmospheric pressure plasma-induced graft polymerization for multifunctional protective clothing, Journal of Polymer Science Part B: Polymer Physics 50 (2012) 1165–1172.

[24] D Sun, X Chen, Plasma modification of Kevlar fabrics for ballistic applications, Textile Reseach Journal 82 (2012) 1928–1934.

[25] M Ferraris, S Perero, M Miola, S Ferraris, E Verné, J Morgiel, Silver nanocluster–silica composite coatings with antibacterial properties, Materials Chemistry and Physics 120 (2010) 123-126.

[26] M Ferraris, S Perero, M Miola, S Ferraris, G Gautier, G Maina, G Fucale, E Verne, Chemical, mechanical, and antibacterial properties of silver nanocluster–silica composite coatings obtained by sputtering, Advanced engineering materials 12 (2010) B276-B282.

[27] M Ferraris, C Balagna, S Perero, M Miola et al., Silver nanocluster/silica composite coatings

obtained by sputtering for antibacterial applications, IOP Conf. Series: Materials Science and Engineering 40 (2012).

[28] M Ferraris, S Ferraris, M Miola, S Perero et al., Effect of thermal treatments on sputtered silver nanocluster/silica composite coatings on soda-lime glasses: ionic exchange and antibacterial activity, Journal of Nanoparticle Research 14 (2012) 1-19.

[29] C Balagna, S Perero, S Ferraris, M Miola et al., Antibacterial coating on polymer for space application, Materials Chemistry and Physic 135 (2012) 714-722.

[30] G Muzio, S Perero, M Miola, M Oraldi et al., Biocompatibility versus peritoneal mesothelial cells of polypropylene prostheses for hernia repair, coated with a thin silica/silver layer, Journal of Biomedical Materials Research Part B: Applied Biomaterials 105 (2016) 1586-1593.

[31] F Baino, S Ferraris, M Miola, S Perero et al., Novel antibacterial ocular prostheses: Proof of concept and physico-chemical characterization, Materials Science and Engineering 60 (2016) 467-474.

[32] NCCLS M2-A9, Performance Standards for Antimicrobial Disk Susceptibility, Approved Standard, ninth ed., (2006).

[33] T.J Franz, Percutaneous absorption on the relevance of in vitro data, J. Invest. Dermatol. 64 (1975) 190-195.

[34] C Bianco, G Adami, M Crosera, F Larese, S Casarin, C Castagnoli, M Stella, G Maina, Silver percutaneous absorption after exposure to silver nanoparticles: a comparison study of three human skin graft samples used for clinical applications, Burns 40 (2014) 1390-1396.

[35] J Davies, R.J Ward, J.R Heylings, Multi-species assessment of electrical resistance as a skin integrity marker for in vitro percutaneous absorption studies, Toxicol. in Vito 18 (2004) 351-358.

[36] UNI 8279-4:1984, Nonwovens- Test methods- Determination of tensile strength (Grab Test), (1984).

[37] UNI 9073-4, Textiles e Test Methods for Nonwovens e Determination of Tear Resistance, (1999).

[38] UNI 12947-2:2000, Textiles- Determination of the abrasion resistance of fabrics by the Martindale method, (2000).

[39] S Davidovic, M Miljković, V Lazić, D Jović, B Jokić, S Dimitrijević, M Radetić, Impregnation of cotton fabric with silver nanoparticles synthesized bydextran isolated from bacterial species Leuconostoc mesenteroides T3, Carbohydrate Polymers 131 (2015) 331-336.

[40] Y Wang, C Yan, C Li, Z Lu, C Ma, Y Yan, Y Zhang, Charge Transfer Tuned by the Surrounding Dielectrics in TiO2-Ag Composite Arrays, Nanomaterials 8 (2018) 1-9.

[41] N.Y Hebalkar, S Acharya, T.N Rao, Preparation of bi-functional silica particles for antibacterial and self cleaning surfaces, Journal of Colloid and Interface Science 364 (2011) 24-30.

[42] B Tomsic, B Simončič, B Orel, L Černe et al., Sol–gel coating of cellulose fibres with antimicrobial and repellent properties, J Sol-Gel Sci Technol, 47 (2008) 44-57.

[43] K Jamuna-Thevi, S.A Bakar, S Ibrahim, N Shahab, M.R.M Toff, Quantification of silver ion release, in vitro cytotoxicity and antibacterial properties of nanostuctured Ag doped TiO_2 coatings on stainless steel deposited by RF magnetron sputtering, Vacuum 86 (2011) 235-241.

[44] M Irfan, S Perero, M Miola, G Maina, A Ferri, M Ferraris, C Balagna, Antimicrobial functionalization of cotton fabric with silver nanoclusters/silica composite coating via RF co-sputtering technique, Cellulose 24 (2017) 2331–2345.

[45] C Balagna, M Irfan, S Perero, M Miola, G Maina, D Santella, A Simone, Characterization of antibacterial silver nanocluster/silica composite coating on high performance Kevlar® textile, Surface & Coatings Technology 321 (2017) 438–447.

[46] S.Y.C Tong, J.S Davis, E Eichenberger, T.L Holland, V.G Fowler, Staphylococcus aureus infections: epidemiology, pathophysiology, clinical manifestations, and management, Clin Microbiol Rev. 28 (2015) 603-661.

[47] A.M Mittelman, J.D Fortner, K.D Pennell, Effects of ultraviolet light on silver nanoparticle mobility and dissolution, Environmental Science Nano 2 (2015) 683-691.

[48] Y Li, W Zhang, J Niu, Y Chen, Surface coating–dependent dissolution, aggregation, and ROS generation of silver nanoparticles under different irradiation conditions, Environmental Science & Technology 47 (2013) 10293–10301.

[49] C Bianco, S Kezic, M Crosera, V Svetličić, S Šegota, G Maina, C Romano, F Larese, G Adami, In vitro percutaneous penetration and characterization of silver from silver-containing textiles, International Journal of Nanomedicine 10 (2015) 1899–1908.

[50] F.F Larese, F D'Agostin, M Crosera, G Adami, N Renzi, M Bovenzi, G Maina, Human skin penetration of silver nanoparticles through intact and damaged skin, Toxicology 255 (2009) 33–37.

[51] X Cheng, K Ma, R Li, X Ren, T.S Huang, Antimicrobial coating of modified chitosan onto cotton fabrics, Applied Surface Science 309 (2014) 138–143.